



Reduction Mechanism of Thermally Stable CaO during Heating Mg-Al Composites with CaO Particles

Junko Umeda¹, Junji Fujita¹, Shufeng Li², Katsuyoshi Kondoh^{1*}

¹Joining and Welding Research Institute, Osaka University, 11-1 Mihogaoka, Ibaragi, Osaka 567-0047, Japan

²School of Materials Science & Engineering, Xi'an University of Technology, Xi'an 710048, China

*Corresponding author. kondoh@jwri.osaka-u.ac.jp (K. Kondoh)

Abstract Mg-6wt%Al-1wt%Zn-0.3wt%Mn alloy powder composite precursors with CaO additive particles were prepared by using an equal channel angular bulk mechanical alloying process. The precursors were annealed at 400-500 °C to synthesize fine Al₂Ca second phases by a solid-state reaction between a Mg-Al matrix and CaO additives. X-ray diffraction revealed that CaO additives were thermally decomposed and solid-soluted Ca atoms diffused into the α -Mg matrix in the Mg-Al-CaO precursors with both 2.5 and 10.0-vol% CaO particles after the heat treatment. Their solid-solution and diffusion were accelerated by heating temperature, heating time, and CaO content. X-ray diffraction, scanning electron microscopy-energy-dispersive spectroscopy and electron probe micro-analysis clarified that the Ca atoms in α -Mg solid solution were immediately saturated in the precursors with 10.0-vol% CaO particles due to the large amount of Ca atoms supplied from CaO. As a result, Al₂Ca formation occurred after a short heat treatment. Al₂Ca were transformed into (Mg,Al)₂Ca after a long heat treatment at 500 °C. In the case of the precursors with 2.5-vol% CaO particles, the solid-soluted Ca atoms slowly increased. As a result, Al₂Ca intermetallic precipitates were formed after a long heat treatment at 450 °C or more.

Keywords Magnesium, Powder metallurgy, Phase transitions, Heat treatment, Reduction behavior

1. Introduction

Magnesium alloys are effective for weight reduction in automotive structural components due to the low density of Mg $\sim 1.74\text{g/cm}^3$, where their use is expected to help increase fuel efficiency [1-4]. It is necessary to improve the heat resistance of Mg alloys without raising the material cost for their widespread use in automotive power train components such as engine blocks and transmission cases used at elevated temperatures (120-200 °C) [4-6]. Previous studies have reported that the addition of calcium to Mg-Al cast alloys had an important benefit in improving the creep resistance at the above temperature range [7-9]. This is because network-structural intermetallic compounds such as Al₂Ca or (Mg,Al)₂Ca were formed around the α -Mg grain boundaries. On the other hand, these network-structural compounds potentially cause grain boundary fractures. Fine dispersed particles of intermetallic compounds are more effective at suppressing grain boundary fractures and improving the yield stress of Mg alloys via pinning effects.

In the present study, CaO particles are employed as raw materials to disperse fine Al₂Ca particles in an α -Mg matrix via a solid-state reaction between CaO particles and the Mg-Al alloy. Conventional Mg-Al alloys reinforced with fine Al₂Ca particles are expected to demonstrate excellent creep resistance and yield stress. They are also expected to be low cost materials because of the use of inexpensive CaO particles as raw materials. However, from a thermodynamic point of view, the Ellingham diagram of the oxide formation [10] indicates that CaO reduction by Mg never occurs in the solid state (up to 650 °C). Therefore, the CaO raw particles should remain in the cast Mg material. On the other hand, our previous study [11] reported that CaO



reduction with Al_2Ca and MgO formation occurred in $\text{Mg-6wt\%Al-1wt\%Zn-0.3wt\%Mn}$ (AZ61B) instead of pure Mg because the change in the standard free energy became negative. Another study [12] revealed that, in the AZ61B composite precursor with 10.0-vol% CaO particles, Ca atoms originating from CaO were solid-soluted in the α -Mg matrix and diffused along the α -Mg grain boundaries. Al atoms solid-soluted in the α -Mg matrix also diffused to the grain boundaries by attracted to the Ca atoms because of a strong combination of Al and Ca elements. As a result, needle-like $(\text{Mg,Al})_2\text{Ca}$ intermetallics were formed as intermediate precipitates during the initial stage of the heat treatment. Finally, they were transformed into the spherical Al_2Ca compounds by the substitution of Al atoms for Mg atoms in $(\text{Mg,Al})_2\text{Ca}$ after a long heat treatment, as shown in Figure 1 [11,12].

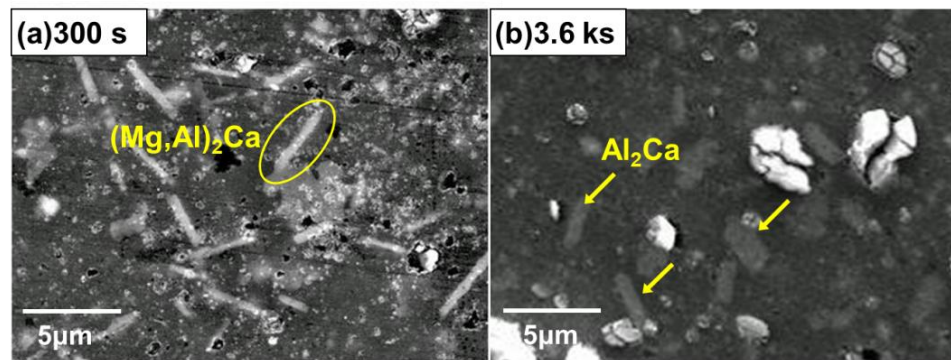


Fig.1 SEM micrographs of the Mg-Al-CaO precursors with 10.0-vol% CaO particles after the heat treatment at 500 °C for 300 s (a) and 3.6 ks (b).

Nevertheless, the reactivity of the Al_2Ca solid-state synthesis is not completely clear. The above reaction mechanism suggests that Al_2Ca formation occur in the all Mg-Al-CaO precursors regardless of CaO content because all of the CaO particles contact the Mg-Al alloy matrix. By contrast, according to the experimental result shown in Fig. 2 [11], the Al_2Ca synthesis was promoted by the increase of CaO additive particles. In particular, no Al_2Ca was detected in the Mg-Al-CaO precursor with 2.5-vol% CaO particles below 500 °C. This reason cannot be well-explained only by the CaO reduction behavior.

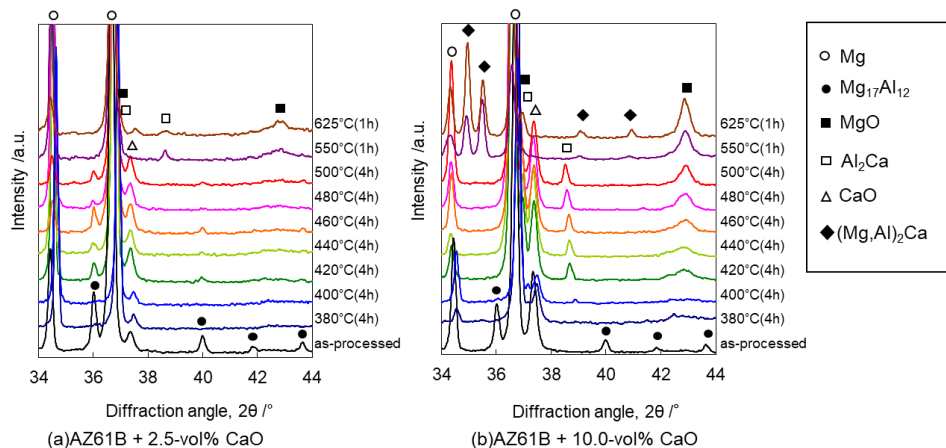


Fig.2 XRD profiles of the Mg-Al-CaO precursors in as-ECABMA state and after the heat treatment. The content of the CaO additives was 2.5-vol.% (a) and 10.0-vol% (b).

In this study, the formation mechanism of Al-Ca or Al-Ca-Mg intermetallic compounds via a solid-state reaction of CaO additives dispersed in an AZ61B powder composite precursor during the heat treatment was investigated in detail by scanning electron microscopy (SEM), electron probe micro-analysis (EPMA), and X-ray diffraction (XRD) analysis. The effect of the heating condition on the microstructures and these intermetallics synthesis was clarified by XRD, SEM-energy-dispersive spectrometry (EDS) analysis. Phase identification was carried out through compositional analysis by EPMA. Finally, the thermally stable phases were investigated using an isothermal section of the Al-Mg-Ca ternary phase diagram.



2. Materials and Methods

2.1. Preparation of AZ61B precursors containing CaO particles

AZ61B chips machined from their original cast ingot (Al; 6.41, Zn; 1.02, Mn; 0.28, Si; 0.02, Fe; 0.004, Cu; 0.002, Ni; 0.0007, Mg; Bal./mass%) were employed as raw materials. They had a mean particle size of 1.38 μm as measured by a particle size analyzer (HORIBA, LA-950). CaO particles for use as additives, having a mean particle size of 2.3 μm , were prepared from CaO blocks with a purity of 98% or more via mechanical fragmentation using a ball milling process. The elemental mixtures of the AZ61B chips and CaO particles were mixed by rocking mill equipment (SeiwaGiken Co., RM-05S) and used as the starting materials. The content of the CaO additives was 2.5 and 10.0-vol%. The AZ61B green compacts containing CaO particles were subjected to severe plastic working by an equal-channel angular bulk mechanical alloying (ECABMA) process [13], where cold compaction and extrusion within a channel bent were alternately carried out in the die, as illustrated in Fig. 3. The maximum compaction pressure was 611MPa. The ECABMA process was repeated 50 times in total resulting in the homogeneous dispersion of the CaO additive particles in the AZ61B alloy chip matrix. This process was also effective for the mechanical breakage of the MgO surface oxide films of the AZ61B chips and resulted in the formation of newly created Mg active surfaces of the chips that directly came into contact with the CaO particles. The green compact billet (Mg–Al–CaO precursor) prepared by the above process had a 35-mm diameter and an 80-mm length.

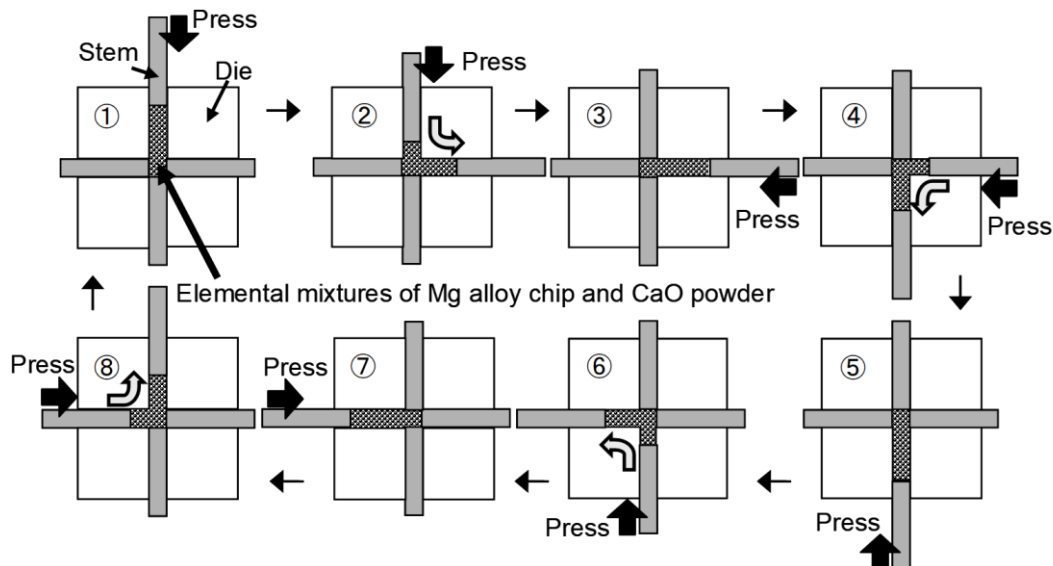


Fig.3 Schematic illustration of one cycle of equal channel angular bulk mechanical alloying (ECABMA) process used in fabrication of Mg alloy powder precursor containing CaO particles [11,12].

2.2. Heat treatment of AZ61B composite precursor with CaO particles

The precursor was heat treated at 400, 450 and 500°C in an argon gas atmosphere in order to investigate the reaction behavior between the AZ61B matrix and the CaO particles. The heating time was 300s, 14.4ks and 86.4ks.

2.3. Microstructural analysis

X-ray diffraction analysis (Shimadzu, XRD-6100) was used to clarify the crystal structure of the α -Mg matrix and identify the synthesized precipitate. The chemical composition of the precipitate distributed in the matrix of the precursor was investigated by an electron probe micro-analyzer (JEOL, JXA-8530F). A field emission scanning electron microscope (JEOL, JSM-6500F) equipped with an energy-dispersive X-ray spectrometer (JEOL, EX-64175 JMU) was used to investigate the microstructures of the heat treated precursors.

3. Results and Discussion

3.1. Microstructural analysis after heat treatment

Microstructural changes of the Mg–Al–CaO precursors with 2.5 and 10.0-vol% CaO particles were investigated by applying a heat treatment for 86.4 ks. The heating temperatures were 400, 450 and 500°C. Fig. 4 shows XRD



patterns of the Mg–Al–CaO precursors after the heat treatment. In the case of the Mg–Al–CaO precursors with 10.0-vol% CaO particles, unknown peaks of a precipitate different from Al_2Ca were detected after the heat treatment at 500 °C. According to Fig.2 (d), Al_2Ca precipitates were formed in the same precursor after the heat treatment at 500 °C for 14.4 ks. This indicates that thermally stable phases changed by a long heat treatment. On the other hand, the Al_2Ca phase was detected after the heat treatment at 400 and 450 °C. In the case of the precursors with 2.5-vol% CaO particles, Al_2Ca formation also occurred by the heat treatment at 450 and 500°C.

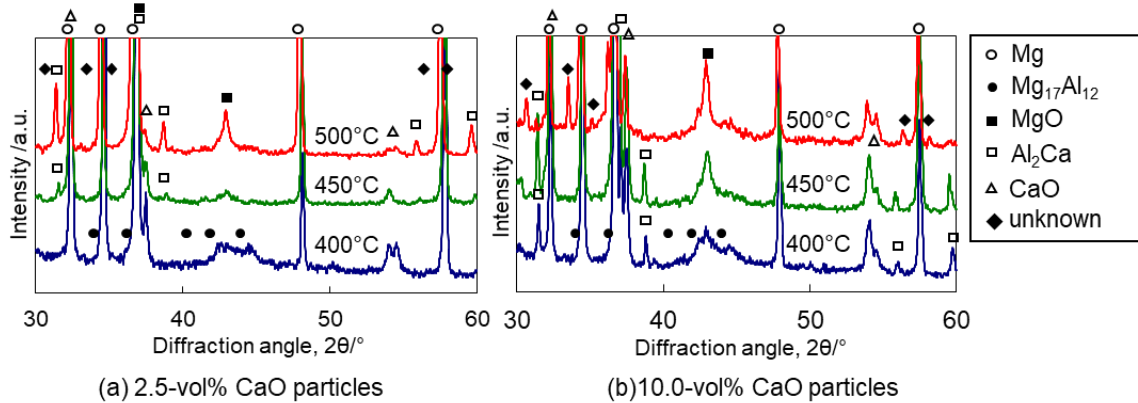


Fig.4 XRD profiles of the Mg–Al–CaO precursors after the heat treatment at 400, 450 and 500 °C for 86.4 ks. The content of the CaO additives was 2.5-vol.% (a) and 10.0-vol% (b).

Figure 5 shows SEM-EDS analysis result of the Mg–Al–CaO precursor with 2.5-vol% CaO particles after the heat treatment at 450 °C for 86.4 ks. Fine and spherical Al_2Ca precipitates and CaO particles were dispersed in the α -Mg matrix. This means that not all CaO particles were decomposed in this heat treatment condition. In conclusion, Al_2Ca formation can occur in the Mg–Al–CaO precursors with both 2.5 and 10.0-vol% CaO particles. However, the progress of the Al_2Ca synthesis was promoted by increasing heating temperatures, heating time and CaO content as seen in Fig. 2 and Fig. 4. This is possibly because a higher number of Ca atoms were dissolved and diffused in α -Mg matrix.

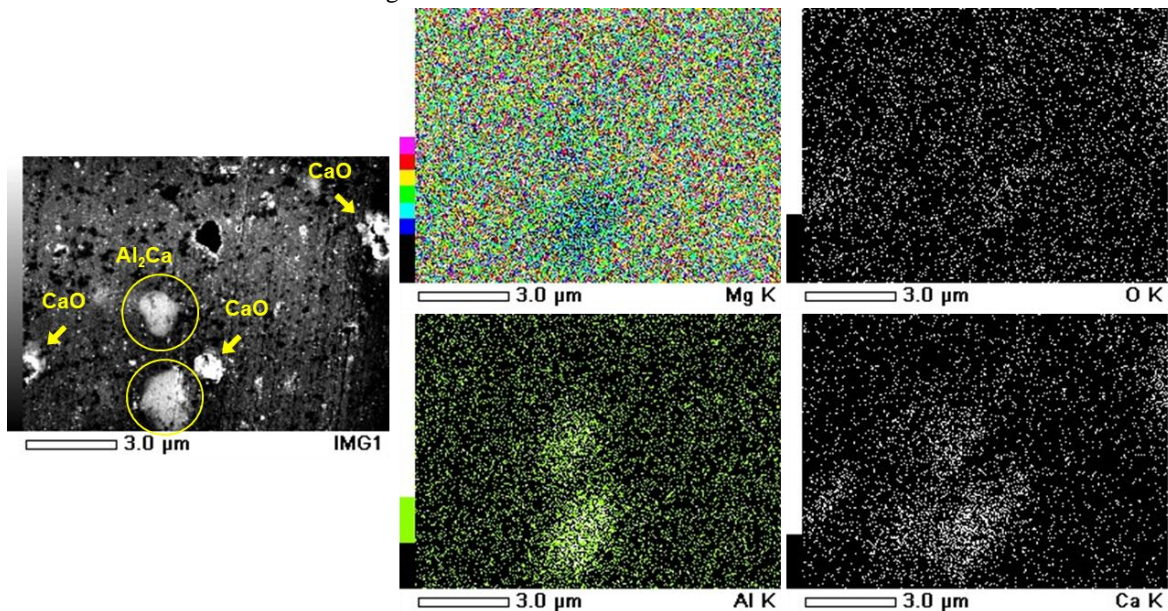


Fig.5 SEM-EDS mapping analysis result of the Mg–Al–CaO precursor with 2.5-vol% CaO particles after the heat treatment at 450 °C for 86.4 ks.

3.2. α -Mg crystal structure change by solid-solution

The crystal structural analysis of the α -Mg phase in the Mg–Al–CaO precursors was carried out in order to investigate the solid-solution behavior of Al and Ca atoms in the α -Mg matrix during the heat treatment. Figure 6 shows XRD analysis on the Mg–Al–CaO precursors with 2.5 and 10.0-vol% CaO particles in the as-processed



state (before heat treatment) and after the heat treatment at 500 °C. The heating time was 300 s, 14.4 ks and 86.4 ks.

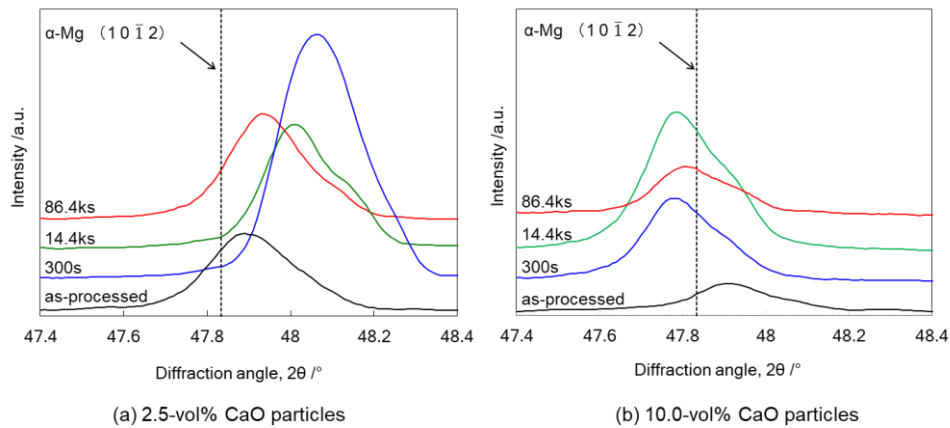


Fig.6 XRD profiles of the Mg-Al-CaO precursors in as-processed state and after the heat treatment at 500 °C for 300s, 14.4ks and 86.4ks. The content of the CaO additives was 2.5-vol.% (a) and 10.0-vol.% (b).

In the case of the precursors with 2.5-vol% CaO particles, the XRD peak of the α -Mg phase in the as-processed state shifted to a higher angle compared to the original peak illustrated by the dotted line ($2\theta=47.83^\circ$). The previous study [12] reported that, in the as-processed precursor, Al atoms existed in the β -phase ($Mg_{17}Al_{12}$), Al_6Mn and a supersaturated solid-solution state in the α -Mg matrix. The above peak shift was caused by the solid-soluted Al atoms. Solid-soluted Al atoms created a smaller lattice spacing in α -Mg because the atomic radius of Al (1.43 Å) is smaller than that of Mg (1.60 Å) [14]. The same peak after the heat treatment at 500 °C for 300 s shifted to a much higher angle. The Mg-Al binary phase diagram [15] suggests that β -phases ($Mg_{17}Al_{12}$) were resolved at over 380°C in the case of the AZ61B alloy (Mg-6.41wt%Al). Therefore, the solid-soluted Al atoms originated from β -phase ($Mg_{17}Al_{12}$) resulted in this peak shift to a higher angle. On the other hand, the same peak after the heat treatment for 14.4 ks shifted to a slightly lower angle compared to that after the heat treatment for 300 s. This indicates that a few Ca atoms originated from CaO were solid-soluted in the α -Mg matrix. Solid-soluted Ca atoms created a larger lattice spacing in α -Mg because of the larger atomic radius of Ca (1.97 Å) compared to that of Mg (1.60 Å) [16]. After the heat treatment for 86.4 ks, the peak shifted to a further lower angle because of both the increase in the number of solid-soluted Ca atoms by the progress of CaO decomposition and the decrease in the number of solid-soluted Al atoms by Al_2Ca formation as shown in Figure 4(a). According to these results, in the Mg-Al-CaO precursors with 2.5-vol% CaO particles, the low distribution density of CaO contributed to the small amount of solid-soluted Ca atoms supplied from CaO. As a result, Ca atoms below the solid solubility limit were solid-soluted in the α -Mg matrix, and no Al_2Ca were formed during the heat treatment for a duration of 14.4 ks or less as shown in Fig. 2 (a). Solid-soluted Ca atoms gradually increased with heating time, and resulted in Al_2Ca formation after a long heat treatment as shown in Fig.4 (a). In the case of the Mg-Al-CaO precursors with 10.0-vol% CaO particles, the XRD peak of the α -Mg phase in the as-processed state also shifted to a higher angle due to the solid-soluted Al atoms. After the heat treatment for 300 s, 14.4 ks and 86.4 ks, the peak shifted to a lower angle compared to the original peak. The angles of these peaks were constant regardless of the heating time. This indicates that the amounts of Al and Ca atoms solid-soluted in the α -Mg matrix were also constant during the heat treatment. This also suggests that, after just a short heat treatment time, such as 300 s, almost all solid-soluted Al atoms contributed to synthesis of Al-Ca or Al-Ca-Mg precipitates, and Ca atoms solid-soluted in the α -Mg matrix were already saturated. This is because the high distribution density of CaO contributed to the large number of solid-soluted Ca atoms supplied from CaO. As a result, the precipitates containing Ca atoms were immediately formed in the initial stage of the heat treatment as shown in Fig. 1. After the initial stage, CaO decomposition contributed not to increasing the amount of solid-soluted Ca atoms but to further precipitation. Therefore, it is estimated that the Ca composition of the precipitates increased and they transformed into other unknown compounds (◆) after the heat treatment at 500 °C for 86.4 ks as shown in Fig. 4 (b). In conclusion, the progress of the Al_2Ca synthesis depended on the



amount of Ca atoms supplied from CaO decomposition into the α -Mg matrix. Therefore, it was promoted by increasing heating temperatures, heating time and CaO content as shown in Fig. 2 and Fig. 4.

3.3. Phase identification by compositional analysis

As shown in Fig. 4 (b), an unknown precipitate different from Al_2Ca was detected after the heat treatment at 500 °C for 86.4 ks in the Mg–Al–CaO precursors with 10.0-vol% CaO particles. It was difficult to identify by using X-ray diffraction. In this section, phase identification of the unknown precipitates shown in Fig. 4 (b) was carried out. Fig. 7 shows SEM observation on Mg–Al–CaO precursor with 10.0vol% CaO particles after heat treatment at 500 °C for 86.4 ks. Bar-like precipitates more than 10 μm length and spherical ones with about 1 μm diameter were observed in α -Mg matrix.

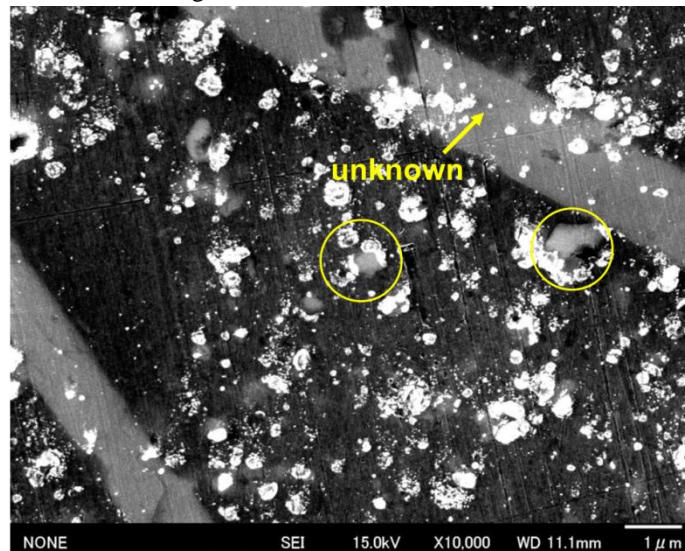


Fig.7 SEM micrographs of the Mg-Al-CaO precursor with 10.0-vol.% CaO particles after the heat treatment at 500 °C for 86.4 ks.

Fig. 8 shows the EPMA mapping and line analysis results for the same precursor. Fig. 8 (a) indicates that the unknown precipitates contained elemental Al and Ca. As shown in Fig. 8 (b), the two unknown precipitates (A and B) each showed different intensities of elemental Mg. This means that their intensities were influenced by the α -Mg matrix around these precipitates. Thus, the Mg composition of the smaller precipitate (A) was higher than that of the larger one (B). On the other hand, Mg, Al and Ca intensities of the area C were constant. This suggests that their intensities were not influenced by the α -Mg matrix. That is, the unknown precipitates possibly contained Mg element, and resulted in a Al-Ca or Mg-Al-Ca intermetallic compounds.

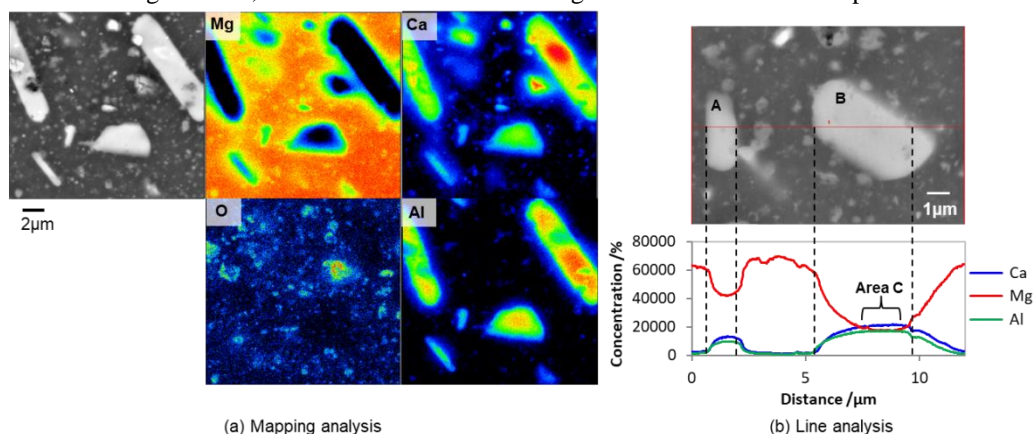


Fig.8 EPMA analysis results of the Mg-Al-CaO precursor with 10.0-vol% CaO particles after the heat treatment at 500 °C for 86.4 ks. Mapping analysis result (a) and Line analysis result (b).

Figure 9 shows EPMA point analysis results of the precipitates. The measurement point was 11. Mg composition showed large variations from measurement points because of the influence of the α -Mg matrix as

mentioned above. The atomic ratio Ca/Al was almost constant as shown in Fig. 9 (a). The mean value was 0.74. This indicates that all of them had the same composition. In addition, Fig. 9 (b) shows that the (Mg+Al)/Ca atomic ratio have a strongly correlation with Mg composition. These results suggests that the variation of (Mg+Al)/Ca atomic ratio was also caused by the detection of the α -Mg matrix. The minimum value of the (Mg+Al)/Ca atomic ratio was about 2. In conclusion, the Mg composition of the precipitate was about 2 or less. Table 1 shows Ca/Al and (Mg+Al)/Ca atomic ratio for Al-Ca and Al-Ca-Mg intermetallics reported in the previous studies [17-18]. According to Fig. 9 and Table 1, the unknown precipitates were identified as (Mg,Al)₂Ca phases. Suzuki et al. [14] reported that the lattice parameters of the (Mg,Al)₂Ca phases have no specific value because of the variable compositions. Thus, it was difficult to identify the (Mg,Al)₂Ca phase by using X-ray diffraction as shown in Fig. 4(b).

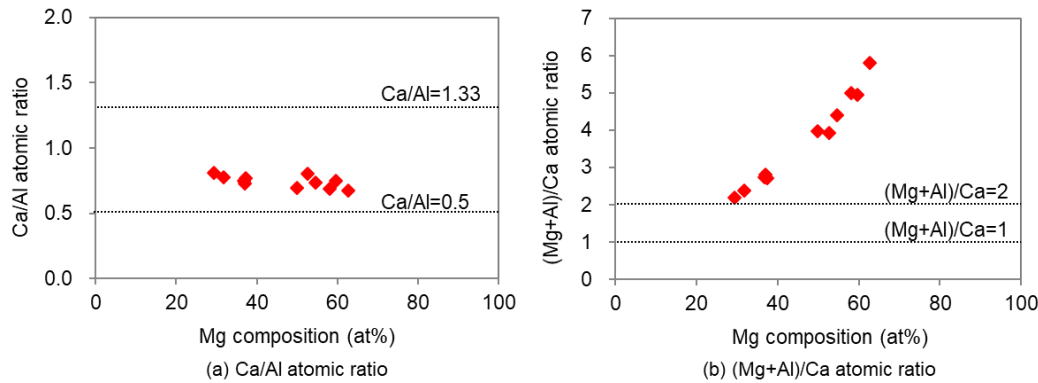


Fig.9 EPMA point analysis results of the unknown precipitates in the Mg-Al-CaO precursor with 10.0-vol% CaO particles after heat treatment at 500 °C for 86.4 ks. Ca/Al atomic ratio (a) and (Mg+Al)/Ca atomic ratio (b).

Table 1 Ca/Al and (Mg+Al)/Ca atomic ratio for Al-Ca or Al-Ca-Mg intermetallic compounds reported in the previous study [17,18].

Atomic ratio	Ca/Al	(Mg+Al)/Ca
Al ₄ Ca	0.25	-
Al ₂ (Ca,Mg)	0.5 or less	2 or more
Al ₂ Ca	0.5	-
(Mg,Al) ₂ Ca	0.5 or more	2
Al ₄ Ca ₁₃	0.93	-
Ca ₄ Al ₃ Mg	1.33	1
Al ₃ Ca ₈	2.67	-

3.4. Consideration of thermally stable phases

The consideration of the thermally stable phase in the Mg–Al–CaO precursors at 500 °C was carried out by using an isothermal section of the Al-Mg-Ca ternary system. Recently, many studies have reported isothermal sections of the ternary system [17,19-21]. However, the thermally stable phase at each temperature was inconclusive. Fig. 10 shows one of them reported by D. Kevorkov et al. [17]. Now suppose that the Mg-Al-CaO precursors were composed of the Al-Mg-Ca ternary alloy matrix and unreacted CaO particles. The matrix in the as-processed state contained 5.9 at% Al originated from AZ61B alloy chips as raw materials. Ca composition in the matrix increased with the progress of CaO decomposition as shown in Fig.10 (b).

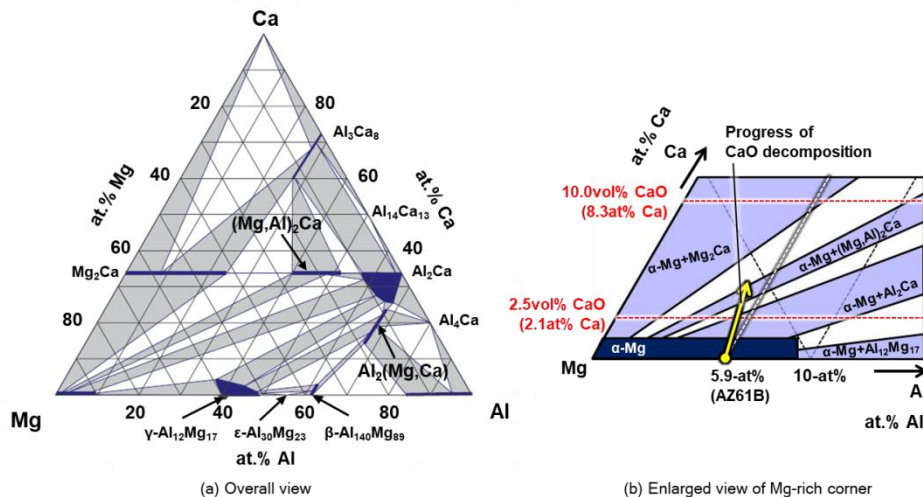


Fig. 10 Isothermal section of the Al-Mg-Ca phase diagram at 400 °C from the literature [17] (a) and the enlarged view of Mg-rich corner (b).

As a result, Al_2Ca intermetallics were formed as thermally stable phases at first. After a longer heat treatment, Ca composition increased further. In case of Mg–Al–CaO precursors with 2.5-vol% CaO particles, the maximum composition of Ca element was 2.1 at% as shown in Fig. 10 (b). When all of CaO particles were decomposed, the alloy composition stayed within the range where the stable phases were $\alpha\text{-Mg}$ and Al_2Ca . Therefore, Al_2Ca phases were formed as thermally stable phases after heat treatment for 86.4 ks. On the other hand, no precipitate was detected after heat treatment for 14.4 ks or less because the Ca composition in the matrix stayed within the solid solubility limit of $\alpha\text{-Mg}$ phase. In case of Mg–Al–CaO precursors with 10.0-vol% CaO particles, the maximum composition of Ca element was 8.3 at%. In addition, the Ca composition of the matrix increased sooner due to the higher distribution density of CaO, compared to that of the precursors with 2.5-vol% CaO particles. As a result, thermally stable Al_2Ca synthesis occurred after a heat treatment of just 14.4 ks. After a longer heat treatment, the Ca composition further increased and the Al_2Ca precipitates were transformed into $(\text{Mg,Al})_2\text{Ca}$ phases as thermally stable phases as shown in Fig. 10 (b).

4. Conclusion

AZ61B powder composite precursors with CaO additive particles prepared via the ECABMA process were heat treated to synthesize Al_2Ca intermetallic precipitates in a solid-state reaction. XRD, SEM-EDS and EPMA were used to investigate changes in the microstructure of heat-treated precursors. Al_2Ca or $(\text{Mg,Al})_2\text{Ca}$ intermetallic precipitates were formed in Mg–Al alloy after a long heat treatment in both of the Mg–Al–CaO precursors with 2.5 and 10.0-vol% CaO particles. Their synthesis was promoted by increasing heating temperatures, heating time and CaO content. This is because higher amount of Ca atoms were solid-soluted and diffused in the $\alpha\text{-Mg}$ matrix. XRD analysis revealed that, in the case of the Mg–Al–CaO precursors with 2.5-vol% CaO particles, solid-soluted Ca atoms gradually increased with heating time and diffused into the $\alpha\text{-Mg}$ grains. As a result, the Al_2Ca synthesis required a long heat treatment at 450 °C or 500 °C. In the case of the precursors with 10.0-vol% CaO particles, the number of solid-soluted Ca atoms immediately increased. Al_2Ca were formed as thermally stable phases after the heat treatment at first. The thermally stable phases changed into $(\text{Mg,Al})_2\text{Ca}$ intermetallics after a long heat treatment because the Ca composition in the $\alpha\text{-Mg}$ matrix increased by the progress of CaO decomposition.

Acknowledgements

The authors would like to thank Keitaro Enami, Masaki Ohara, Takanori Igarashi from TOPY Industries, Limited, for supporting preparation of AZ61B precursors containing CaO particles via ECABMA process. This study was financially supported by both International Joint Research Promotion Program promoted by Osaka University and “Project to Create Research and Educational Hubs for Innovative Manufacturing in Asia,” Osaka



University of the Special Budget Project of the Ministry of Education, Culture, Sports, Science, and Technology.

Conflicts of interest or competing interests

The data required to reproduce these findings cannot be shared at this time due to technical or time limitations.

References

- [1]. M. Gupta, N.M.L. Sharon. (2011). *Magnesium, Magnesium Alloys, and Magnesium Composites*, John Wiley & Sons, New Jersey.
- [2]. USGS. (2015). *Mineral Commodity Summaries*, U.S. Geological Survey, Reston.
- [3]. A. Tharumarajah, P. Koltun. (2017). Is there an environmental advantage of using magnesium components for light-weighting cars?, *J. Clean. Prod.*, 15: 1007-1013.
- [4]. A.A. Luo. (2013). Magnesium casting technology for structural applications, *J. Magn. Alloys*, 1: 2-22.
- [5]. C.J. Bettles, M.A. Gibson, S.M. Zhu. (2009). Microstructure and mechanical behaviour of an elevated temperature Mg-rare earth based alloy, *Mater. Sci. Eng. A*, 505: 6-12.
- [6]. M.O. Pekguleryuz, A.A. Kaya. (2003). Creep Resistant Magnesium Alloys for Powertrain Applications, *Adv. Eng. Mater.*, 5: 866-878.
- [7]. D. Amberger, P. Eisenlohr, M. Göken. (2009). Microstructural evolution during creep of Ca-containing AZ91, *Mater. Sci. Eng. A*, 510-511: 398-402.
- [8]. B. Kondori, R. Mahmudi. (2010). Effect of Ca additions on the microstructure, thermal stability and mechanical properties of a cast AM60 magnesium alloy, *Mater. Sci. Eng. A*, 527: 2014-2021.
- [9]. S.W. Xu, N. Matsumoto, K. Yamamoto, S. Kamado, T. Honma, Y. Kojima. (2009). High temperature tensile properties of as-cast Mg-Al-Ca alloys, *Mater. Sci. Eng. A*, 509: 105-110.
- [10]. H.J.T. Ellingham. (1944). The physical chemistry of process metallurgy, *J. Soc. Chem. Ind.*, 63: 125-133.
- [11]. K. Kondoh, J. Fujita, J. Umeda, H. Imai, K. Enami, M. Ohara, T. Igarashi. (2011). Thermo-dynamic analysis on solid-state reduction of CaO particles dispersed in Mg-Al alloy, *Mater. Chem. Phys.*, 129: 631-640.
- [12]. J. Fujita, J. Umeda, K. Kondoh. (2017). Synthesis of Al₂Ca dispersoids by powder metallurgy using a Mg-Al alloy and CaO particles, *Materials*, 10(7): 716, DOI:10.3390/ma10070716.
- [13]. K. Enami, J. Fujita, Y. Motoe, M. Ohara, T. Igarashi, K. Kondoh. (2008). Development of magnesium alloy composites by bulk mechanical alloying process, *J. Jpn. Soc. Powder Metallurgy*, 55: 244-249.
- [14]. A. Suzuki, N.D. Saddock, J.W. Jones. (2004). T.M. Pollock, Structure and transition of eutectic (Mg,Al)₂Ca Laves phase in a die-cast Mg-Al-Ca base alloy, *Scripta Mater.*, 51: 1005-1010.
- [15]. T.B. Massalski. (1986). *Binary Alloy Phase Diagrams*, vol. 1, American Society for Metals, Metals Park, Ohio.
- [16]. T. Rzychoń, B. Chmiela. (2012). The influence of tin on the microstructure and creep properties of a Mg-5Al-3Ca-0.7Sr-0.2Mn magnesium alloy, *Sol. St. Phen.*, 191: 151-158.
- [17]. D. Kevorkov, M. Medraj, J. Li, E. Essadiqi, P. Chartrand. (2010). The 400°C isothermal section of the Mg-Al-Ca system, *Intermetallics*, 18: 1498-1506.
- [18]. Q.A. Zhang, W.M. Yang, E. Akiba. (2005). Synthesis and crystal structure of a new ternary compound Ca₄Al₃Mg, *J. Alloy. Compd.*, 398: 123-126.
- [19]. A. Suzuki, N.D. Saddock, J.W. Jones, T.M. Pollock. (2006). Phase Equilibria in the Mg-Al-Ca Ternary System at 773 and 673 K, *Metall. Mater. Trans. A.*, 37A: 975-976.
- [20]. A. Janz, J. Grobner, H. Cao, J. Zhu, Y.A. Chang, R. Schmid-Fetzer. (2009). Thermodynamic modeling of the Mg-Al-Ca system, *Acta Mater.*, 57: 682-694.
- [21]. Y. Zhong, J. Liu, R.A. Witt, Y. Sohn, Z. Liu. (2006). Al₂(Mg,Ca) phases in Mg-Al-Ca ternary system: First-principles prediction and experimental identification, *Scripta Mater.*, 55: 573-576.

